

# Production of Charged Pions from Hydrogen and Carbon\*

A. H. ROSENFELD

*Institute for Nuclear Studies, University of Chicago, Chicago, Illinois*

(Received June 4, 1954)

The cross sections and energy spectra of pions produced in the reactions  $P+P\rightarrow\pi^++D$  and  $P+P\rightarrow\pi^++N+P$  have been measured at three angles using 440-Mev protons. Both reactions contribute about equally to the total cross section. The total cross section is  $(4\pm 1)$  mb and the angular distribution is proportional to  $(0.15\pm 0.06+\cos^2\theta)$ .

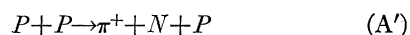
The energy spectra of  $\pi^+$  and  $\pi^-$  produced in a carbon target at  $90^\circ$  in the laboratory system has also been measured. We find  $(d\sigma_{\pi^+}/d\Omega) = (0.83\pm 0.11)$  mb sterad $^{-1}$  per C nucleus and a  $\pi^+/\pi^-$  ratio of  $7.2\pm 1.5$ .

## I. INTRODUCTION

THE total production of pions in  $P$ - $P$  collisions has been studied up to 50 Mev above threshold in the c.m. system.<sup>1</sup> It is of interest to extend the range of these measurements in order to get more information on the excitation function and also to allow direct comparison with the reactions  $N+P\rightarrow\pi^++N$  which are currently being studied using beams from the Chicago synchrocyclotron.

The importance of this excitation function and of this comparison is discussed in reference 1, in which an attempt is made to describe all the cross sections for pion production in nucleon-nucleon collisions in terms of the Watson-Brueckner<sup>2</sup> phenomenological treatment. This treatment assumes the conservation of isotopic spin, which by now has a sound experimental basis.

We have studied pion production 63.7 Mev above threshold in the c.m. system using nuclear emulsions exposed to targets of polyethylene and carbon bombarded by the internal 440-Mev beam of the Chicago synchrocyclotron. The pion energy spectrum and absolute cross section have been measured at three angles. The spectrum consists of a continuum associated with the reaction



and in addition, just above the high-energy cutoff of the continuum, a line associated with



Our results show that reactions (A') and (B) contribute about equally to the cross section and that the pion angular distribution is proportional to  $0.15+\cos^2\theta$ . Our total cross section is  $(4\pm 1)$  mb. Within the large experimental error this agrees with a reasonable extrapolation of the available data, which are compiled and discussed in reference 1.

For the purpose of making the polyethylene-carbon subtraction it is necessary to study the production of  $\pi^+$  in proton-carbon collisions. It was relatively easy to extend the scanning to cover the entire  $\pi^+$  and  $\pi^-$

spectra at an angle of  $90^\circ$  in the laboratory system. Our results are compared with similar data for lower energies. We attempt to interpret the cross section in terms of a model which assumes that pions are produced in collisions between a beam proton and an individual nucleon in carbon. This approach gives agreement with experiment within about 30 percent for the lower half of the spectrum, but fails at higher energy.

## II. EXPERIMENTAL ARRANGEMENT

This experiment was undertaken before a high-intensity proton beam was extracted from the Chicago synchrocyclotron. The low intensity of the scattered external beam made it necessary to work with the circulating beam inside the vacuum chamber, despite difficulties that will be discussed.

The target is a  $\frac{1}{8}$ -inch rod of polyethylene or carbon. The total flux of protons through the target is determined by counting the 20.5-min  $C^{11}$  activity produced in the target. Pions emitted at three downward angles from the target are slowed down in absorber and come to rest in a well-shielded nuclear emulsion.

Immediately after the irradiation the film must be withdrawn from the vacuum chamber so that it will not be fogged by gamma radiation and the target must be withdrawn so that it can be counted. Even after the cyclotron has been standing idle for several hours the general radiation level at the tank walls is  $\sim \frac{1}{2}$  r/hr, so that photographic emulsions cannot be kept there more than a few minutes.

The over-all physical design of the experiment was determined by the largest air-lock available, which was 8 in. long and designed to permit the passage of a 4-inch diameter probe.

Figure 1 shows the target and absorber-emulsion holder. The hinged holder lies horizontal while traversing the air-lock and then falls into the vertical position shown. The absorber was made of "pseudite," a material designed to have the same linear stopping power and "scattering power" as emulsion (see subsection D).

### A. Proton Beam

The energy spectrum under study will be meaningful only if the bombarding proton beam is nearly mono-

\* Work supported in part by the U. S. Atomic Energy Commission and the U. S. Office of Naval Research.

<sup>1</sup> References may be found in Table III of the following paper [A. H. Rosenfeld, Phys. Rev. **95**, 139 (1954)].

<sup>2</sup> K. M. Watson and K. A. Brueckner, Phys. Rev. **83**, 1 (1951).

energetic. We shall describe the Chicago proton beam and how its energy spread was reduced.

A proton spiraling out in an orbit which is almost a perfect circle will hit the target at  $75\frac{1}{2}$ -in. radius when it attains an energy of  $444 \pm 1\frac{1}{2}$  Mev. The energy is calculated from magnetic field measurements, and the uncertainty in this energy arises from the uncertainty as to how well the beam is centered about the axis of the pole faces.

Actually, most protons do not simply spiral out slowly, but rather they oscillate radially and vertically about their stable orbit. At  $75\frac{1}{2}$ -in. radius in our cyclotron the average amplitude of the vertical oscillations is about 0.6 in., and some of the radial amplitudes are greater than 4 in. The vertical oscillations are not serious, but the radial oscillations cause the energy of the protons hitting a target to be decreased by as much as 35 Mev. This comes about because a proton can hit the target when its instantaneous radius is greater than that of its stable orbit.

These radial oscillations were suppressed by placing a vertical 0.1-in. tungsten rod along the magnetic center of the cyclotron, bathed by the ion beam emerging from the arc source. This rod, suggested by R. H. Hildebrand, reduced the radial oscillation to  $<1$  in. (9 Mev);<sup>3</sup> it also reduced the beam intensity by a factor of  $\sim 1000$ . This reduction is no disadvantage for photographic work, since even with this low intensity our exposures took only a few seconds.

During the exposures, oscillograms were taken of the time at which protons hit the target. Since there is an almost unique correspondence between time and proton kinetic energy, these oscillograms can be interpreted to show that all but 8 percent of the protons hitting the target had oscillations corresponding to  $<8$  Mev; the remainder had energy deficiencies rather uniformly distributed between 8 and 32 Mev. These figures apply to the  $90^\circ$  exposures. At the time the irradiations were performed for the other two angles the vacuum was poor and the radial oscillations larger, resulting in an energy spread of 12 Mev.

A proton may make repeated traversals through the target before it is multiply scattered enough to collide with the dee. The proton loses some energy with each traversal, so that unless precautions are taken the beam energy will be degraded over about 20 Mev. We reduced this spread to about 1.5 Mev by placing a "clipper" 0.7 in. below the median plane. About one third of the protons had such large vertical oscillations that they hit the clipper before they ever hit the target, but we were willing to take a 30 percent increase in background in the interest of energy resolution.

The beam was also clipped  $\frac{1}{2}$  in. out radially from the tip of the target. This kept protons from hitting the brass probe tip and making background pions and protons. It also helped reduce multiple traversals, but

<sup>3</sup> A. H. Rosenfeld and S. D. Warshaw, Rev. Sci. Instr. (to be published).

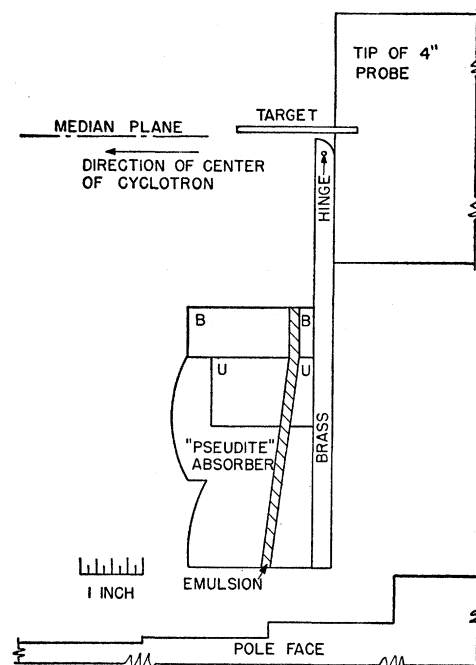


FIG. 1. Target and absorber, side view, looking into the proton beam. The energy of a pion is determined by the distance it goes through absorber before coming to rest in nuclear emulsion. As shown, the absorber will stop pions with energy up to 100 Mev. To investigate higher energies, the pieces of absorber labelled B and U, and the emulsion between them, were replaced with solid pieces of brass and uranium.

radial clipping is rather ineffective for this purpose when there are radial oscillations.

### B. Shielding

The emulsion holder was shielded on three sides by 8 in. of nonradioactive lead. This primary shielding was entirely inadequate protection from protons coming from the beam direction; it was necessary to add another 8 in. of secondary shielding, extending  $\frac{1}{2}$  in. nearer the median plane, so as completely to shield the primary shielding.

### C. Emulsions

The choice of emulsion was governed by several rather severe requirements. It had to be insensitive to unavoidable gamma exposure of about 0.1 r, and yet the meson tracks had to be heavy enough and the variation in grain density near the end of the track rapid enough to produce distinctive  $\pi$ - $\mu$  decays. It was also necessary that the processed emulsion be quite transparent, since a thickness of  $1800\mu$  was desired.

The gamma background ruled out the possibility of using Ilford G5 emulsion, and thick layers of processed C2 or B2 emulsion are often not very transparent. Mr. C. Waller, of Ilford, Ltd., was kind enough to supply us with a new emulsion, G-special, which is similar to G5 except that it has a sensitivity only slightly higher than that of C2. The processed emulsion

was sufficiently clear that mm graph paper could easily be read through it. The variation of grain density near the end of a meson track is sufficiently rapid that a  $\pi$ - $\mu$  decay is easily recognizable; the tracks are heavy enough to allow scanning for  $\pi$ - $\mu$  decays with a 12 $\times$  oil-immersion objective.

Our scanning technique is most efficient with emulsions about 2 mm thick. We used pellicles (emulsion stripped from glass backing) for two reasons—first, 1800- $\mu$  plates are difficult to process if the solutions can penetrate from only one side; secondly, we wished to use the pellicles themselves as part of the absorber; hence the presence of the glass, with its different stopping power for charged particles, was undesirable in an otherwise homogeneous absorber.

### D. Absorber

We wish first to show that the energy of a pion cannot be accurately determined if there is a significant difference between the linear stopping power of the absorber and that of the emulsion. In order to demonstrate this we must consider the multiple scattering of a pion as it slows down.

The pion will deviate from its original line of flight. The root mean square of the deviation projected on a plane which passes through the original line of flight is given by

$$y_{rms} = 0.18R^{0.95} \approx 0.18R,$$

where  $R$  is the range, and all distances are measured in cm. The formula applies for energy  $<100$  Mev. This effect is illustrated in Fig. 2, where the shaded area is a triangle with half-angle 0.18 radian and represents the projection of a cone through which most pions of 90 Mev pass as they slow down. The half-angle is comparable with the angle between the plane of the emulsion and the original pion direction. It is therefore inevitable that some of the pions coming to rest in a thick emulsion will have travelled some considerable

distance through the emulsion rather than through the absorber proper. The thicker the emulsion used, the more stringent is the requirement that the linear stopping power of the absorber be matched to that of emulsion.

The absorber should also be chosen with Coulomb scattering properties close to those of emulsion. This minimizes preferential in- or out-scattering from the emulsion to the absorber. This effect is not quite negligible. For example, a crude estimate shows that if the average  $Z$  of the absorber were 13, even though its stopping powers were equal to that of the emulsion, the density of endings in the emulsion would be reduced by about 5 percent. This correction is uncertain and hard to estimate, and would vary rapidly with position in the emulsion. We preferred to make an absorber, "pseudite," which matches emulsion both in linear stopping power and in radiation length.

### Pseudite

This is a machinable moulded mixture of fine copper, tin, and Lucite powders, 150 mesh or smaller. Each cc of the sample used contains 1.28 g Cu, 1.94 g Sn, and 0.71 g Lucite, and has a total density of  $3.93 \pm 2$  percent. This is actually about 2.5 percent greater than was desired for a perfect match, so that the linear stopping power is 2.5 percent higher than that of emulsion of density 3.83. Pion ranges in pseudite were obtained by using Aron's<sup>4</sup> range-energy tables for Cu, assuming that Cu and pseudite (and emulsion) have the same mass stopping power. This recipe is accurate to 1 percent for pions with energy  $>10$  Mev. It was arrived at by using the average ionization potentials of Mather and Segrè<sup>5</sup> and ignoring multiple scattering, which will be discussed separately in Sec. II-H.

### E. Nuclear Absorption of Pions

We next consider the errors introduced by attenuation of the pions while they are being brought to rest. While traversing the absorber some pions will collide with nuclei and be absorbed. Others will be scattered, and if this scattering angle is  $>40^\circ$  they will probably never be seen during scanning, and if seen they will be discarded.

The top part of Fig. 3 displays a collection of data on the total cross section for  $\pi^\pm$  in nuclear emulsion. At high energy the  $\pi^-$  cross section approaches about 1.3 times geometrical cross section, whereas attenuation cross sections determined using scintillation counters seem to approach geometrical. This discrepancy need not concern us because of our large statistical error for  $\pi^-$  (we found only 25  $\pi^-$ ). The solid curves which merge with the geometrical cross section at high energy represent the cross sections assumed for the purpose of computing attenuation.

<sup>4</sup> W. A. Aron, University of California Radiation Laboratory Report UCRL-1325, 1951 (unpublished).

<sup>5</sup> R. Mather and E. Segrè, Phys. Rev. 84, 191 (1951).

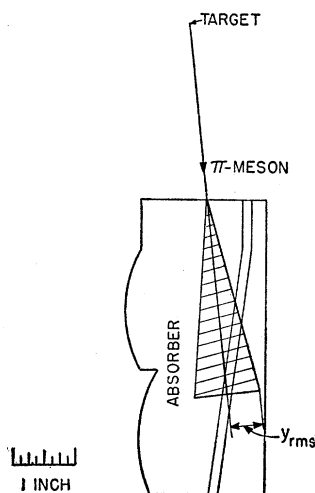


FIG. 2. Scattering of a 90-Mev pion as it comes to rest in emulsion. The shaded area indicates the region most probably traversed by the pion.

The bottom part of the figure shows the computed attenuation. The corrections for losses are small (5.5 percent for the highest energy pion which can come from hydrogen at  $90^\circ$ , and less than 30 percent for the  $55^\circ$  case) so some error in the assumed cross section produces a negligible error in our final result.

## F. Irradiation and Monitoring

The number of protons hitting the carbon and  $\text{CH}_2$  targets was determined by counting the  $\text{C}^{11}$  nuclei formed in the target. The cross section for the reaction  $\text{C}^{12}(p, pn)\text{C}^{11}$ ,  $(41 \pm 3)$  mb at 440 Mev as measured by Rosenfeld, Swanson, and Warshaw,<sup>6</sup> was adopted.

The targets were monitored by slipping them into a positron-to-gamma converter with wall thickness just sufficient to stop the 0.95-Mev positrons from  $\text{C}^{11}$ . The annihilation radiation escaping from the converter was counted with a Geiger counter. An absolute ( $\pm 1$  percent)  $4\pi$  flow counter, kindly lent by V. L. Telegdi, was used to determine the efficiency of monitoring; this was  $1.70 \times 10^{-3}$  with a precision of 1 percent.

TABLE I. Effect upon pion energy resolution of multiple scattering, spread in beam energy, and straggling.

Laboratory angle	$55^\circ$	$90^\circ$	$124^\circ$
Spread <sup>a</sup> due to			
Imperfect angular resolution	8.0	3.0	0.5
Spread in proton beam energy	3.35	1.42	1.50
Straggling	1.40	0.76	0.44
Multiple scattering	2.25	1.25	0.67
Total spread	9.15	3.63	1.73

<sup>a</sup> Standard deviation, measured in Mev, of a Gaussian in the laboratory system.

A suitable exposure produced from  $5 \times 10^6$  to  $130 \times 10^6$   $\text{C}^{11}$  nuclei and took only a few seconds. The statistical error in monitoring was  $\approx 1$  percent, which is smaller than the other errors of about 2 percent introduced by uncertainties in time measurements, geometry, etc.

## G. Energy Resolution

The theoretical energy spectrum for  $P+P \rightarrow \pi^+$  is sketched at the bottom of Fig. 6. It consists of a continuum populated mainly at the high-energy end and then, a few Mev above the high-energy cutoff, a line associated with the production of bound deuterons [reaction (B)]. We wish to discuss in order of decreasing importance three experimental effects which will broaden the line so that it overlaps the continuum.

### 1. Angular Resolution

Because of the multiple scattering illustrated in Fig. 2, a pion coming to rest on a line making a given angle with the proton beam may have been emitted at a slightly different angle. The angular spreads are as

<sup>6</sup> Rosenfeld, Swanson, and Warshaw (to be published).

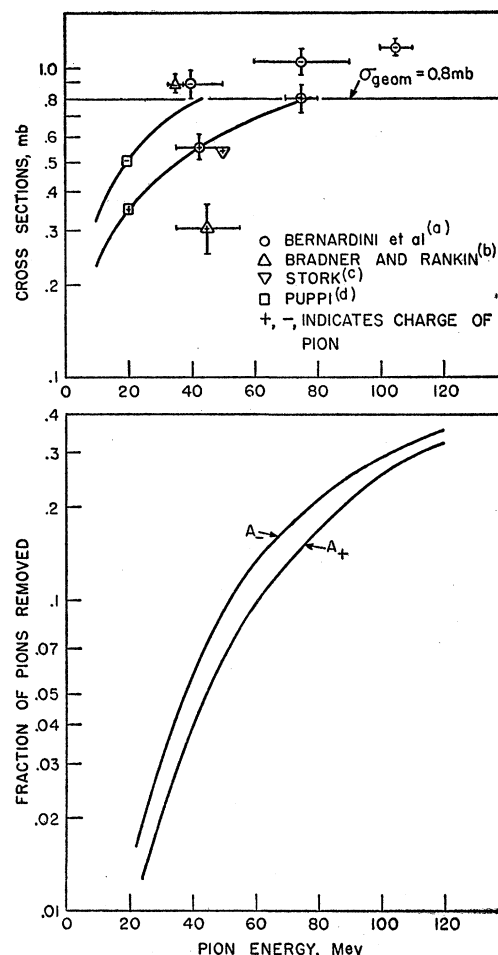


Fig. 3. Total cross section and attenuation of pions in emulsion. The crosses represent observed total cross sections in nuclear emulsion; the smooth curves are the cross sections assumed for computing the attenuation. The curves  $A_+$  and  $A_-$  at the bottom give the computed attenuation for  $\pi^+$  and  $\pi^-$ .

### References:

- <sup>a</sup> G. Bernardini, Booth, and Lederman, Phys. Rev. **83**, 1075 (1951); **84**, 610 (1951).
- <sup>b</sup> H. Bradner and B. Rankin, Phys. Rev. **87**, 547 (1952).
- <sup>c</sup> D. H. Stork, Phys. Rev. **92**, 538 (1953).
- <sup>d</sup> G. Bernardini (private communication).

follows: for the exposure at  $55^\circ$ , half-width  $5.15^\circ$ ; for  $90^\circ$ ,  $3.2^\circ$ ; for  $124^\circ$ ,  $1.3^\circ$ . In the laboratory system the energy of a pion emitted in reaction (B) is a sensitive function of the angle at which it is observed. The first row of Table I gives the energy spread arising from the angular spread. This spread could be reduced if it were possible to place the absorber farther from the target, but this was ruled out by the 8-in.-long air-lock.

### 2. Spread in the Initial Proton Energy

A spread in the energy of the proton beam causes spread in pion energy which depends upon the angle at which the pion is observed. This latter spread is given in the second row of Table I.

### 3. Scattering and Straggling

These last sources of energy spread are inherent to the process of slowing down; they would be present even if it were possible to run the experiment with a monochromatic external proton beam.

For pions, straggling is not as important as the loss in resolution due to multiple scattering. Measured ranges are shortened 5 percent on the average because they are only projections of longer paths with wiggles in them. The value 5 percent applies for pion energies up to 100 Mev, and for emulsion. The distribution of shortened ranges is not Gaussian,<sup>7</sup> but we treat it as such. The loss in energy resolution resulting from the spread in range is shown in Table I. We used a range-energy relation which was corrected to take into account the average 5 percent shortening of the measured range as compared with the true range.

### III. CALCULATION OF THE CROSS SECTION

The number of pions of energy  $T$  observed coming to rest in a volume  $ds \cdot dx$  is

$$dn = 0.982 N_H J \frac{d^2\sigma}{d\Omega dT} \frac{ds}{x^2} \frac{dT}{dx} \times [1 - A(T)](1 + \delta)(1 - \epsilon). \quad (1)$$

The factor 0.982 is the probability that a pion shall not decay in flight. For our geometry this probability is remarkably independent of pion energy.  $N_H$  is the effective target thickness in atoms of H per cm<sup>2</sup>.  $J$  is the number of protons passing through the target;  $x(T)$  is the distance from the target at which the pion comes to rest in emulsion;  $ds$  is an element of area perpendicular to the pion orbit;  $A(T)$  is the fractional attenuation of pions as they pass through the absorber, as given in Fig. 3;  $\delta$  is a small correction arising from the focussing of orbits in the magnetic field of the cyclotron; it is almost independent of  $T$ ;  $\epsilon$  is the

difference of the scanning efficiency from unity (it is small; see Sec. IV).

For pions produced by  $P$ - $P$  collisions in polyethylene,  $(CH_2)_n$ ,  $N_H J$  can be re-expressed as  $2N_{11}/\sigma_{11}$ . Here  $N_{11}$  is the number of  $C^{11}$  nuclei produced during the bombardment and  $\sigma_{11}=41$  mb is the cross section for  $C^{11}$  production.

Equation (1) may now be written

$$\frac{d^2\sigma}{d\Omega dT} = (1 - \delta + \epsilon) \frac{1}{N_{11}K(x)} \frac{dn}{dv}(x), \quad (2)$$

where

$$K(x) = 0.982 \cdot \frac{2}{\sigma_{11}} \cdot \frac{1}{x^2} \cdot \frac{dT}{dx} (1 - A),$$

and  $dx \cdot ds$  has been called  $dv$ .

$$\delta_{55^\circ} = 0.0425, \quad \delta_{90^\circ} = 0.0146, \quad \delta_{124^\circ} = 0.047.$$

The functions  $dT/dx$  and  $x(T)$  were computed assuming a 5 percent shortening of range by projection.

### IV. SCANNING

The emulsions were scanned for the endings of both pions and muons using either 12 $\times$  or 22 $\times$  oil-immersion objectives. Our microscopes were adapted so that it was easy to confine scanning to the middle third of an emulsion originally 1800  $\mu$  thick. This insured that whenever a  $\pi$ - $\mu$  decay was found it was possible to follow the muon to the end of its range,  $(597 \pm 28)\mu$ , and thus identify the event unambiguously in less than a minute.

#### Scanning Efficiency

Another advantage of scanning a thick layer is that it permits a truly objective test of scanning efficiency. If a  $\pi$ - $\mu$  decay is found in the layer of emulsion comprising the middle third of the pellicle, there is about a 50 percent probability that the associated muon will also end in the layer, though not necessarily in the strip currently being scanned. Similarly about one-half of the muon endings observed should lead back to pions in the same layer. Thus pions are found in two independent ways—by direct scanning and via muons; the same applies to muons. If the scanning efficiency were 100 percent it should never happen that a pion is seen only by tracking the corresponding muon, and is missed by direct search. The scanning efficiency for pions found by direct scanning is then given by  $1 - \epsilon = 1 - N_{\text{missed}}/N_{\text{tracked}}$ , where  $N_{\text{missed}}$  is the number of pions missed by direct observation but found by tracking, and  $N_{\text{tracked}}$  is the total number of pions found by tracking. We also kept a similar check on scanning efficiency for muons. As an example we give the result for the 90° exposures. About 200 pions and 200 muons were tracked;  $N_{\text{missed}}$  was 3 pions and 5 muons. We conclude that the scanning efficiency is 98½ percent for pions, 97½ percent for muons.

The greatest advantage to this running efficiency

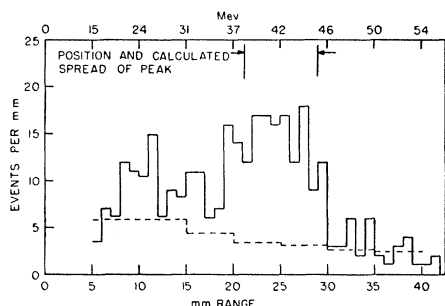


FIG. 4.  $\pi^+$  endings per mm range at 90° lab. The solid histogram represents pions from polyethylene; the dashed one, which has been smoothed by grouping the data, represents the contribution from carbon. The calculated position and experimental spread of the line associated with deuterium formation is taken from Table I.

<sup>7</sup> M. F. Cartwright, Richman, Whitehead, and Wilcox, Phys. Rev. 91, 677 (1953).

TABLE II. Cross section in mb/sterad for pion with c.m. kinetic energy between 50 and 75 Mev. Errors are statistical standard deviations.

$\theta_{c.m.}$	90°	127°	152°
$\theta_{lab}$	55°	90°	124°
$(d\sigma/d\Omega)_{lab}$	$0.12 \pm 0.04$	$0.21 \pm 0.02$	$0.16 \pm 0.03$
$(d\sigma/d\Omega)_{c.m.}$	$0.08 \pm 0.03$	$0.30 \pm 0.03$	$0.48 \pm 0.09$

check is that one can learn to scan rapidly at an efficiency very slightly less than unity and not waste time scanning too carefully.

### Scanning Rate

Near the peaks in the range distribution corresponding to deuterium formations, the number of pions and proton endings is comparable. An experienced scanner can find and identify an ending in 10 minutes.

### V. PION PRODUCTION FROM HYDROGEN—EXPERIMENTAL RESULTS

The results are most interesting after transformation to the c.m. system, but we first present the data in the laboratory system. Three angles were studied.

#### 90° Lab

Figure 4 is a histogram of the data. It shows that the carbon subtraction introduces no serious complication, particularly at the high-energy end of the spectrum, which contributes most to the cross section. Figure 4 also illustrates an internal check on the validity of the subtraction. This check is based on consideration that it is kinematically impossible for the hydrogen in polyethylene to contribute to the production of pions with a range of more than 30 mm. At greater ranges the histogram from polyethylene and carbon should agree within experimental error. In the range from 30 to 55 mm we indeed found 50  $\pi^+$  from polyethylene, 59 from carbon.

Only 15 percent of the cross section from hydrogen lies below 25 Mev, which corresponds to about 12-mm range. At ranges smaller than 12 mm a reduced area of emulsion was scanned, so that only about two-thirds as many events were actually found as are indicated. The statistical errors shown have been appropriately corrected.

Figure 5 (top) gives the data converted to  $d^2\sigma/(d\Omega dT)$ .

#### 124° Lab

No histogram is shown, but Fig. 5 (bottom) gives the cross section per steradian-Mev.

#### 55° Lab

The cross section is small at this angle, which corresponds to 90° c.m. Moreover the peak in the hydrogen spectrum falls at an energy where the carbon spectrum is a maximum. No attempt was made to obtain a

meaningful energy distribution. However, enough pions were found to establish the cross section per steradian given in Table II.

### Transformation to the c.m. System

The transformation from lab. angle to c.m. angle does not depend strongly upon pion energy. Thus at 90° lab. the energy of the high-energy pions associated with deuteron production is 45 Mev, and the corresponding c.m. angle is 127°; for 30-Mev pions, 90° lab. corresponds to 131°; for 10 Mev, 144°. It can be seen that the pion-energy dependence of the transformation can be neglected, particularly since most of the cross section is concentrated in a peak at the high-energy end of the pion spectrum and there are experimental angular spreads of a few degrees arising from multiple scattering and from the fact that a finite volume of emulsion was scanned. The conversion from laboratory angle to c.m. angle was therefore taken to be that for pions of energy corresponding to the deuteron peak.

In Fig. 6 the lab. cross sections of Figs. 5 are transformed to the c.m. system. This transformation is easily calculated by making use of the fact that the quantity  $(1/p)(d^2\sigma/d\Omega dT)$  is an invariant. Here  $p$  stands for the meson momentum.

It can be seen that about half the endings are found in the region where we would expect to find the experimentally spread line spectrum associated with deuteron formation. This is also true of the third angle.

In Sec. VI we shall estimate what fraction of the spectrum is really a line, but first we discuss the results

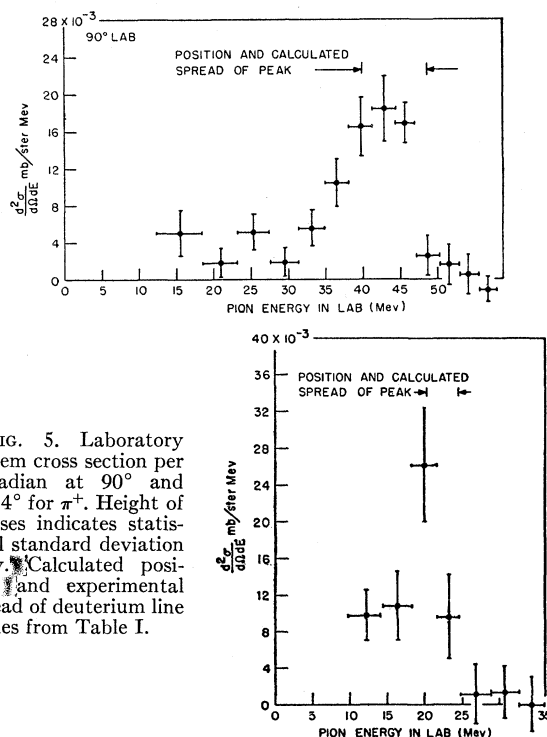


FIG. 5. Laboratory system cross section per steradian at 90° and 124.4° for  $\pi^+$ . Height of crosses indicates statistical standard deviation only. Calculated position and experimental spread of deuteron line comes from Table I.

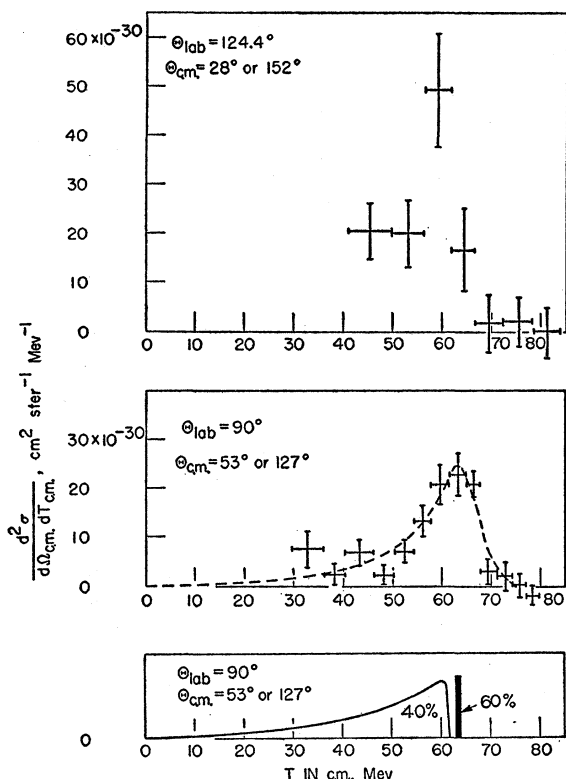


FIG. 6. Pion energy spectra in the c.m. system. These are the data of Figs. 5 converted to the c.m. system. The continuum and line spectrum at the bottom of the figure is the theoretical spectrum for pions accompanied by  ${}^3S$  nucleons. The dashed line plotted along with the  $90^\circ$  lab. data is this theoretical spectrum folded in with the experimental resolution at  $90^\circ$ . (See Sec. VI.)

strictly empirically. At each angle there is a definite peak in the observed pion spectrum in the c.m. energy range 50 to 75 Mev; moreover this peak seems to represent roughly the same fraction of the cross section at that angle, independent of angle. In the peak there is relatively little error introduced by the need for subtracting the pions originating from carbon rather than from hydrogen, whereas this is not true for the rest of the spectrum. For these reasons above we discuss the peak alone. Table II gives the cross section per steradian for pions with c.m. energy between 50 and 75 Mev.

### Angular Distribution

We are describing the collision of identical particles, so the c.m. angular distribution of the pions produced must be symmetric about  $90^\circ$ . With at most 65.4 Mev available to the pion, we assume that only  $s$  and  $p$  final states are important.

The angular distribution must then be of the simple form

$$(d\sigma/d\Omega)_{c.m.} = B(A + \cos^2\theta).$$

A least-squares fit of this function to the data in Table II gives  $A = 0.15 \pm 0.06$ ,  $B = (0.56 \pm 0.09)$  mb/sterad.

These errors are still only statistical. The fit is shown in Fig. 7.

Most of the experimental errors already discussed increase the uncertainty in  $B$  much more than in  $A$ . The 8 percent error in the  $C^{11}$  cross section is the largest single error, but we have assumed that all experimental errors amount to 10 percent. Combining these errors we find for pions with c.m. kinetic energy between 50 and 75 Mev,

$$(d\sigma/d\Omega)_{c.m.} = (0.63 \pm 0.12)(0.15 \pm 0.06 + \cos^2\theta) \text{ mb/sterad.}$$

Integration over solid angle yields

$$\sigma_{50-75 \text{ Mev}} = (3.4 \pm 0.5) \text{ mb.} \quad (3)$$

### VI. ANALYSIS OF THE SPECTRUM

We return to the problem of estimating the total cross section knowing only the partial cross section from 50 to 75 Mev c.m. We had hoped also to estimate the cross section corresponding to the deuteron line, but our conclusions are too ambiguous to be of value.

We shall use the phenomenological considerations described in reference 1. There it is shown that at the energy of our experiment the final nucleons are usually in  $S$  states, with  ${}^3S$  about 10 times more probable than  ${}^1S$  (in the notation of reference 1,  $\sigma_{10} \approx 10\sigma_{11}$  at  $\eta=1$ ). It is further shown that the formation of unbound  ${}^3S$  nucleons relative to bound  ${}^3S$  nucleons (deuterons) should be in the ratio 4:6 almost independent of angle. We have plotted at the bottom of Fig. 6 the predicted spectrum (continuum+line) for pions accompanied by  ${}^3S$  nucleons. This spectrum, along with a similar spectrum representing the small  ${}^1S$  contribution, has been folded into the calculated experimental resolution, and the result is plotted as a dashed line along with the  $90^\circ$  lab. data of Fig. 6. We have attempted to fit only the  $90^\circ$  data since this is the exposure that was most thoroughly scanned. In folding we took into account that during the exposure 92 percent of the protons were in the nominal energy interval  $(440 \pm 4)$  Mev, but that the remaining 8 percent had energies from 408 to 436 Mev, spread about evenly.

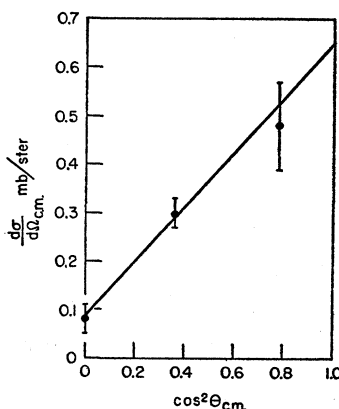


FIG. 7. Cross section per steradian vs  $\cos^2\theta$ . The solid line is a least-squares fit.

The height of the folded curve has been adjusted so that in the c.m. energy interval 50 to 75 Mev the area under the curve agrees with the experimental cross section. The agreement between the experimental spectrum and the folded curve is within statistical error, although if the continuum-to-line ratio had been arbitrary we would have chosen a somewhat larger fraction for the continuum,  $(50 \pm 16)$  percent of the total cross section rather than the value 40 percent obtained from phenomenological considerations.

If we assume that the theoretical spectrum is correct, we can calculate that the total cross section (including the pions associated with  $^1S$  nucleons) is  $(4.0 \pm 0.8)$  mb, and the cross section for deuteron formation is  $(2.0 \pm 0.5)$  mb.

These results may be compared with similar results at other energies, which are displayed in Fig. 3 of reference 1. It can be seen that our total cross section  $(4.0 \pm 0.8)$  mb is in agreement with other results, but the value of 2 mb for deuteron formation does not agree with the other cross sections, which show that the correct value can hardly be more than 1.4 mb at our energy ( $\eta=1.06$ ). We conclude that if there is no gross error in our experiment then the ratio of unbound to bound nucleons formed must be considerably greater than suggested by the phenomenological treatment; our data would suggest almost a factor two.

In reference 1 we show that other experiments do indeed indicate that the unbound-to-bound ratio is higher than predicted; but it is not clear from the evidence presented there whether the phenomenological treatment is inadequate, or whether the extra unbound nucleons are simply nucleons formed in  $P$  states, which we have neglected.  $P$ -state nucleons will be associated with low energy pions, and in our experiment the unexpected pions all have energy greater than 50 Mev, leaving less than 15 Mev for the nucleons. Hence we do not believe that the discrepancy can be fully resolved by invoking  $P$ -state nucleons.

In the light of the discussion above, we cannot state a cross section for the production of pions associated with deuterons, but our value of  $(4.0 \pm 0.8)$  mb for the total cross sections is still meaningful. The fraction of pions with energy less than 50 Mev certainly depends upon the ratio of unbound-to-bound nucleons formed, but we have assumed that this fraction is only 23 percent (see Fig. 6) so that even a fairly serious error in the unbound-to-bound ratio will not seriously affect our estimate for the total cross section.

We must increase the uncertainty in our value for the total cross section to allow for errors in going from the partial cross section above 50-Mev pion energy to the total cross section; we then find

$$\sigma(P+P \rightarrow \pi^+ + \text{nucleons}) = (4 \pm 1) \text{ mb},$$

where nucleons may be either bound or unbound and may be in any angular momentum state.

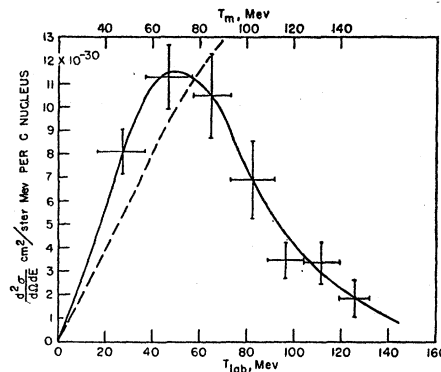


FIG. 8. Energy spectrum of  $\pi^+$  from carbon at  $90^\circ$  lab. A smooth solid line has been drawn through the data. The scale at the top of the figure and the dashed curve refer to the discussion of Sec. VIII.

### VII. PION PRODUCTION FROM CARBON—EXPERIMENTAL RESULTS

The cross section per Mev per steradian for  $\pi^+$  production per C nucleus is shown in Fig. 8. No energy spectrum is given for  $\pi^-$  production. We scanned for  $\pi^-$  endings, but in a volume containing 250  $\pi^+$  endings we found only 25  $\pi^-$  stars. Their energy distribution seems qualitatively to be similar to that for  $\pi^+$ . In order to state the total cross section for  $\pi^-$  production, the number of  $\pi^-$  stars found with one or more prongs was multiplied by 1.37 to account for zero-prong stars.<sup>8</sup>

It was necessary to correct the data for pions which did not originate in the target. Below 100 Mev this background amounted to less than 5 percent, but above 100 Mev its relative importance increases with energy and it becomes as large as the production from the target by 135 Mev. If we were to repeat the experiment we would use a larger target which could increase the signal-to-background ratio by perhaps four and still impair the energy resolution very little.

Including a 10 percent uncertainty for systematic error, we find, for  $\pi^+$  production at  $90^\circ$  lab.,

$$d\sigma/d\Omega = (0.83 \pm 0.11) \text{ mb/sterad per C nucleus.}$$

Production of  $\pi^-$  is lower by a factor  $7.2 \pm 1.5$ , so that

$$d\sigma/d\Omega = (0.11 \pm 0.03) \text{ mb/sterad per C nucleus.}$$

### VIII. PION PRODUCTION FROM CARBON, DISCUSSION

Figure 9 gives the available data (including our own) on the production of pions from carbon as a function of bombarding proton energy. It is of interest to compare this with the analogous excitation functions for the production of pions in nucleon-nucleon collisions; these are given in Fig. 3 of the accompanying paper.<sup>1</sup>

<sup>8</sup> F. I. Adelman and S. B. Jones, Phys. Rev. **75**, 1468 (1949). An independent determination of the fraction of 0-prong stars was made by W. F. Fry and the author. This corroborated Adelman *et al.*



The nucleons in carbon have internal kinetic energy, and this raises the cross section at low bombarding energy,<sup>9</sup> so that the carbon excitation function is less steep than that for hydrogen. The general features illustrated in reference 1 are still present, however, in the sense that the cross section for  $\pi^-$  production is much smaller than that for  $\pi^+$  and probably increases more rapidly with energy.

The authors who report the carbon data of Fig. 9 also report on the production of pions in nucleon-nucleon collisions under the same conditions. The cross sections are combined in Table III to give carbon-to-hydrogen and  $\pi^+/\pi^-$  ratios.

### Analysis in Terms of Nucleon-Nucleon Collisions

This model is similar to that used by Passman, Block, and Havens.<sup>10</sup> It assumes that the bombarding proton interacts with only one nucleon in the target nucleus and that the main effect of the other nucleons is to have given the struck nucleon a momentum distribution. Of course the other nucleons may scatter the incoming proton<sup>11</sup> and the outgoing pion.

We have computed the dashed curve of Fig. 8 using this model with the following assumptions.

1. The momentum distribution of the nucleons is Gaussian, and the mean kinetic energy is 24 Mev.<sup>12</sup>
2. Provided that the maximum energy  $T_m$  available to the pion in the appropriate c.m. system is less than

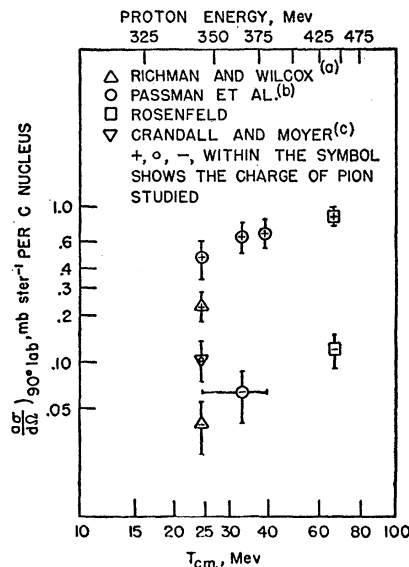


FIG. 9. Excitation function for pions produced at 90° lab. from carbon bombarded with protons. References: (a) G. Richman and H. A. Wilcox, Phys. Rev. **78**, 496 (1950); (b) Passman, Block, and Havens, Phys. Rev. **88**, 1247 (1952); (c) W. E. Crandall and B. J. Moyer, Phys. Rev. **92**, 749 (1953).

<sup>9</sup> W. McMillan and E. Teller, Phys. Rev. **72**, 1 (1947).

<sup>10</sup> Passman, Block, and Havens, Phys. Rev. **88**, 1247 (1952).

<sup>11</sup> S. Gasiorowicz, Phys. Rev. **93**, 843 (1954).

<sup>12</sup> Cladis, Hess, and Moyer, Phys. Rev. **87**, 425 (1952).

TABLE III. Carbon-to-hydrogen and positive-to-negative ratios for pions produced in proton-carbon collisions as a function of bombarding energy.  $T_{c.m.}$  would be the c.m. energy of a pion produced in the reaction  $p+p \rightarrow \pi^+ + d$  if the target nucleon were stationary.

$T_{c.m.}$ , Mev	29.5	29.5-38	63.7
$\frac{d\sigma_C^+}{d\Omega}$	$8 \pm 3$	$11 \pm 1$	$3.6 \pm 0.7$
$\frac{d\sigma_H}{d\Omega}$			
$\frac{d\sigma^+}{d\Omega}$	$5.1 \pm 1.0$	$10 \pm 3$	$7.25 \pm 1.5$
$\frac{d\sigma^-}{d\Omega}$			

100 Mev, then  $\sigma(P+P \rightarrow \pi^+)$  is given by the dashed line in Fig. 3 of reference 1. We ignore  $P-N$  collisions. For simplicity we make the entirely unjustified assumption that each pion is created with energy  $0.8T_m$ . The angular distribution is proportional to  $0.2 + \cos^2\theta_{c.m.}$  (see reference 1).

3. If a pion is scattered or absorbed as it leaves the nucleus it will not be seen at 90° lab. We used the interaction cross sections reported by Stork.<sup>13</sup>

Although about one-half of the incoming protons will be scattered by carbon, we ignored this possibility, but we did take into account the suppression of  $\pi^+$  production by Coulomb repulsion.

It can be seen that the computed curve falls below the experimental results at low energy, and above for  $T_m > 80$  Mev. There appear to be two main reasons for this:

1. The reduction of energy of incident protons due to scattering will tend to reduce high-energy and increase low-energy pion production.
2. Our approximation of representing the pion spectrum in the reaction  $(P+P \rightarrow \pi^+ + \text{nucleon})$  by a  $\delta$  function obviously underestimates the number of low-energy pions.

We have not attempted to extend the calculation beyond 100 Mev because the extrapolation from lower energies of both the cross section  $\sigma(P+P \rightarrow \pi^+)$  and the pion absorption mean free path becomes quite dubious.

It might be noted that when data on  $P+P \rightarrow \pi^+$  at high energies become available one might be able to solve for the absorption mean free path, a quantity which is not easily accessible to direct measurement.

### IX. CONCLUSIONS AND ACKNOWLEDGMENTS

In 440-Mev  $P-P$  collisions, pions are produced with a differential and total cross section which is in fair agreement with extrapolation of the lower-energy results. Both the lower-energy data and ours indicate that the fraction of pions produced along with bound deuterons is lower than predicted by the phenomeno-

<sup>13</sup> D. H. Stork, Phys. Rev. **93**, 868 (1954).

logical theory of Brueckner and Watson. This is discussed in reference 1.

We wish to thank Professor E. Fermi for his continued help. S. B. Treiman assisted greatly in the design of the experiment, and W. E. Slater and F. T. Solmitz con-

tributed valuable help. Thanks are due to J. E. Boyce of the Argonne National Laboratory for the loan of the uranium absorber. We are indebted to the entire cyclotron staff, and to the scanners, Enid Bierman, J. T. Lach, and W. E. Slater, for their cooperation.

PHYSICAL REVIEW

VOLUME 96, NUMBER 1

OCTOBER 1, 1954

## Production of Pions in Nucleon-Nucleon Collisions at Cyclotron Energies

A. H. ROSENFELD

*Institute for Nuclear Studies, University of Chicago, Chicago, Illinois*

(Received June 7, 1954)

All available data on the production of pions in nucleon-nucleon collisions at cyclotron energies are compiled and are compared with the phenomenological theory of Watson and Brueckner. The principle of conservation of isotopic spin allows all these cross sections to be written in terms of only three independent cross sections, whose excitation functions are predicted by the phenomenological model. The theory represents satisfactorily the excitation functions and the angular distributions that are known experimentally; however the experimental ratio  $\sigma(P+P \rightarrow \pi^+ + N+P)/\sigma(P+P \rightarrow \pi^+ + D)$  appears to be about a factor 2 larger than predicted.

Using a notation for total cross section in which the first subscript indicates the isotopic spin of the initial state, and the second that of the final state of the two nucleons, and expressing all cross sections in millibarns, we find:

$$\begin{aligned}\sigma_{10}(D) &= \sigma(P+P \rightarrow \pi^+ + D) &= 0.14\eta + 1.0\eta^3, \\ \sigma_{10}(N+P) &= \sigma(P+P \rightarrow \pi^+ + N+P) - \sigma_{11} \approx 1.5\eta^4, \\ \sigma_{01} &= 2\sigma(N+P \rightarrow \pi^\pm) - \sigma_{11} &\lesssim 0.3\eta^4, \\ \sigma_{11} &= \sigma(P+P \rightarrow \pi^0) &\approx 0.2\eta^3.\end{aligned}$$

$\eta$  is the maximum c.m. momentum available to the pion, measured in units of  $\mu c$ .

### I. INTRODUCTION

IN 1951 several authors<sup>1-3</sup> succeeded in interpreting satisfactorily the data then available on the production of pions near threshold. The only reaction that had been studied extensively was  $P+P \rightarrow \pi^+ + D$ , mainly using 340-Mev protons, corresponding to a pion energy of 22 Mev in the c.m. system. By assuming that the pions are created mainly in  $p$  states and by treating the nucleon-nucleon interaction phenomenologically it was possible to explain the energy spectrum and angular distribution of the pions, and to predict the excitation function for the reaction.

Since 1951 the information available on pion production has been greatly extended.<sup>4</sup> There are now data on  $N-P$  as well as  $P-P$  collisions; the energy range studied has been extended downwards to 10 Mev above threshold (where  $s$ -state production of pions should become relatively important) and cross sections have been published up to 50 Mev above threshold. Currently the Pittsburgh and Chicago synchrocyclotrons are being used to study the energy region 46 to 92 Mev. At Chicago eight experiments either are in progress or else have been recently completed.

There is by now some experimental confirmation of the principle of conservation of isotopic spin in pion production.<sup>5-7</sup> According to this principle it is possible to express all pion production data for each energy in terms of only three independent differential cross sections;<sup>3</sup> moreover the phenomenological treatment makes certain predictions about the excitation functions for these cross sections. We mean "phenomenological" to include the assumption of charge independence and also all the selection rules that will be discussed below.

We shall show that the new data are consistent with the phenomenological model, even when the pions are relativistic. The only appreciable discrepancy is that the experimental ratio  $\sigma(P+P \rightarrow \pi^+ + N+P)/\sigma(P+P \rightarrow \pi^+ + D)$  seems to be about twice as large as predicted.

We have compiled the available cross sections for pion production in nucleon-nucleon collisions at cyclotron energies, and we have adjusted unknown parameters in the phenomenological treatment so as to give a best fit to the data.

Several authors<sup>8,9</sup> have proposed that various reactions could be sorted out by polarization experiments.

<sup>1</sup> K. Brueckner, Phys. Rev. **82**, 598 (1951).

<sup>2</sup> Chew, Goldberger, Steinberger, and Yang, Phys. Rev. **84**, 581 (1951).

<sup>3</sup> K. M. Watson and K. A. Brueckner, Phys. Rev. **83**, 1 (1951).

<sup>4</sup> References to all experiments are given in Table III.

<sup>5</sup> R. H. Hildebrand, Phys. Rev. **89**, 1090 (1953).

<sup>6</sup> R. A. Schluter, Phys. Rev. **95**, 639(A) (1954).

<sup>7</sup> R. H. Hildebrand and A. H. Rosenfeld (to be published).

<sup>8</sup> K. M. Watson and C. Richman, Phys. Rev. **83**, 1256 (1951).

<sup>9</sup> R. E. Marshak and A. M. L. Messiah, Nuovo cimento **11**, 337 (1954).